A Letters Journal Exploring the Frontiers of Physics

June 2007

EPL, **78** (2007) 57002
doi: 10.1209/0295-5075/78/57002

www.epljournal.org

Novel self-sustained modulation in superconducting stripline resonators

E. Segev[(a)], B. Abdo, O. Shtempluck and E. Buks

Department of Electrical Engineering, Technion - Haifa 32000, Israel

received 23 January 2007; accepted in final form 17 April 2007
published online 16 May 2007

PACS 74.40.+k – Fluctuations (noise, chaos, nonequilibrium superconductivity, localization, etc.)
PACS 85.25.Am – Superconducting device characterization, design, and modeling

Abstract – We study thermal instability in a driven superconducting NbN stripline resonator integrated with a microbridge. A monochromatic input drive is injected into the resonator and the response is measured as a function of the frequency and amplitude of the drive. Inside a certain zone of the frequency-amplitude plane the system has no steady state, and consequently self-sustained modulation of the reflected power off the resonator is generated. A theoretical model, according to which the instability originates by a hotspot forming in the microbridge, exhibits a good quantitative agreement with the experimental results.

Nonlinear effects in superconductors are important for both basic science and technology. A strong nonlinearity may be exploited to demonstrate some important quantum phenomena in the microwave domain, such as quantum squeezing [1–3] and experimental observation of the so-called dynamical Casimir effect [4]; whereas technologically, these effects may allow some intriguing applications such as bifurcation amplifiers for quantum measurements [5,6] and resonant readout of qubits [7].

In this work we study the response of a superconducting (SC) microwave stripline resonator to a monochromatic injected signal. We find that there is a certain range of driving parameters, in which a novel nonlinear phenomenon emerges, and self-sustained modulation (SM) of the reflected power off the resonator is generated by the resonator. That is, the resonator undergoes limit-cycle oscillations ranging between several to tens of megahertz. A theoretical model which attributes the SM to a thermal instability yields a good agreement with the experimental results. A similar phenomenon was briefly reported in the '60s [8–11] in dielectric resonators which were partially coated by a SC film, but it was not thoroughly investigated and therefore its significance was somewhat overlooked. This phenomenon is of a significant importance as it introduces an extreme nonlinear mechanism, which is by far stronger than any other nonlinearity observed before in SC resonators [12]. It results in high intermodulation gain, substantial noise squeezing, period doubling of various orders [12], and strong coupling between resonance modes.

Our device (figs. 1(b)-(d)) integrates a narrow microbridge into a SC stripline ring resonator. The impedance of the microbridge strongly affects the resonance modes of the resonator and thus its resonance frequencies can be tuned by either internal (Joule self-heating) or external (infrared illumination [13]) perturbations [14]. Further design considerations, fabrication details as well as resonance modes calculation can be found elsewhere [13]. The experiments are performed using the setup depicted in fig. 1(a). The resonator is driven by a monochromatic tone at an angular frequency ω_{p}, and the reflected power is measured by a spectrum analyzer in the frequency domain and an oscilloscope in the time domain. Measurements are carried out while the device is fully immersed in liquid helium.

Figure 2 shows typical experimental and numerical results of the SM phenomenon in the frequency domain. The resonator is driven at the resonance frequency of the third mode f_3, and the dependence of the SM on the pump power at the input of the resonator is investigated. At relatively low and relatively high input power ranges ($P_{\mathrm{pump}} \lesssim -33.25$ dBm $\cup$ $P_{\mathrm{pump}} \gtrsim -23.7$ dBm) the response of the resonator is linear, namely, the reflected power contains a single spectral component at the frequency of the driving pump tone ω_{p}. In between these power ranges, regular SM of the reflected power occurs (see panel (b), subplots (ii), (iv)). It is manifested by rather strong and sharp sidebands, which extend over several hundred megahertz at

(a) E-mail: segeve@tx.technion.ac.il

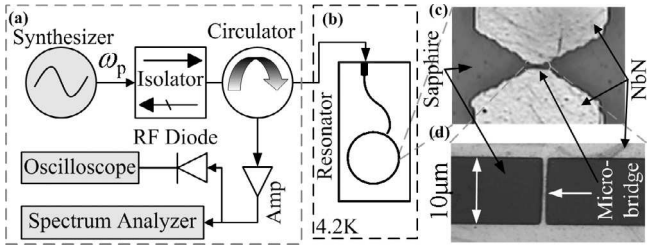

Fig. 1: (a) SM measurement setup. (b) Schematic layout of the device. The resonator is designed as a stripline ring, having a characteristic impedance of 50 Ω. It is composed of 200 nm thick NbN deposited on a sapphire wafer. A weakly coupled feedline is employed for delivering the input and output signals. An optical microscope image of the ring resonator section at which the microbridge is integrated is seen in panel (c), whereas panel (d) shows the microbridge, whose dimensions are $1 \times 10\,\mu\mathrm{m}^2$.

both sides of the resonance frequency. The SM frequency, defined as the frequency difference between the pump and the first sideband, increases with the pump power. The SM starts and ends at two power thresholds, referred to as the lower and the upper power thresholds. The lower power threshold (panel (b), (i)) spreads over a very narrow power range of approximately 10 nW, during which the resonator experiences a strong amplification of the noise floor (noise rise) over a rather large frequency band, especially around the resonance frequency itself. This noise rise can be explained in terms of nonlinear dynamics theory, as it predicts the occurrence of strong noise amplification near a threshold of instability [15,16]. The upper power threshold (panel (b), (vi)) spreads over a slightly larger power range than the lower one and has similar, but less extreme characteristics.

The SM nonlinearity is also strongly dependent on the pump frequency. This dependence is shown in the supplementary video 1 (see footnote [1]), where each frame is a graph similar to fig. 2(a), and corresponds to a different pump frequency, starting at a red-shifted pump frequency ($\Delta f_{\mathrm{pump}} = f_{\mathrm{pump}} - f_3 < 0$) and ending at a blue-shifted pump frequency ($\Delta f_{\mathrm{pump}} > 0$). Figure 3 plots the SM frequency as a function of the pump frequency and power. The inset plots the stability diagram of the resonator (to be discussed below) as a function of the same parameters. The SM occurs only within a well-defined frequency range around the resonance frequency. A small change in the pump frequency can abruptly ignite or quench the SM. Once started though, the modulation frequency has a weak dependence on the pump frequency. The maximum SM frequency measured with this device is approximately 41 MHz, whereas a higher maximum of approximately 57 MHz has been measured with other devices [17].

[1] Typical experimental results of the self-modulation dependence on both the power and frequency of the stimulating monochromatic pump tone. Each frame plots a color-map of the reflected power as a function of the pump power and the measured frequency, centered on the resonance frequency. The frames are obtained while gradually increasing the pump power.

We propose a theoretical model according to which the SM originates from a thermal instability in the microbridge section of the stripline resonator. Current-carrying superconductors are known to have two or more metastable phases sustained by Joule self-heating [18]. One is the SC phase and the other is an electro-thermal local phase, known as hotspot, which is basically an island of normal-conducting (NC) domain, with a temperature above the critical one, surrounded by a SC domain. A perturbation can trigger or suppress the formation of a hotspot and thus, the microbridge can oscillate between the two phases. Such oscillations were often observed in experiments, for the case of a SC microbridge driven by an external dc voltage (see review [18] and references therein).

In the current case, as the microbridge is integrated into a stripline resonator, the system is driven into instability via externally injected microwave pump tone. We herein briefly present the corresponding theoretical model, whereas the full derivation of the equations, as well as experimental justifications to several assumptions are included elsewhere [17]. Consider a resonator driven by a weakly coupled feed-line carrying an incident coherent tone $b^{\mathrm{in}} e^{-i\omega_{\mathrm{p}} t}$, where b^{in} is constant complex amplitude ($\left|b^{\mathrm{in}}\right|^2 \propto P_{\mathrm{pump}}$) and $\omega_{\mathrm{p}} = 2\pi f_{\mathrm{pump}}$ is the driving angular frequency. The mode amplitude inside the resonator can be written as $Be^{-i\omega_{\mathrm{p}} t}$, where $B(t)$ is a complex amplitude which is assumed to vary slowly on a time scale of $1/\omega_{\mathrm{p}}$. In this approximation, the equation of motion of B reads [2]

$$\frac{\mathrm{d}B}{\mathrm{d}t} = \left[i\left(\omega_{\mathrm{p}} - \omega_0\right) - \gamma\right] B - i\sqrt{2\gamma_1} b^{\mathrm{in}} + c^{\mathrm{in}}, \qquad (1)$$

where $\omega_0(T)$ is the temperature-dependent angular resonance frequency, T is the temperature of the hotspot, $\gamma(T) = \gamma_1 + \gamma_2(T)$, where γ_1 is the coupling coefficient between the resonator and the feed-line and $\gamma_2(T)$ is the temperature-dependent damping rate of the mode. The term c^{in} represents an input Gaussian noise with a zero-mean and a random phase. We consider a case where the nonlinearity originates from a local hotspot in the microbridge. If the hotspot is assumed to be sufficiently small, its temperature T can be considered as homogeneous. The temperature of other parts of the resonator is assumed to be equal to that of the coolant $T_0 = 4.2\,\mathrm{K}$. The power Q_{t} heating up the hotspot is given by $Q_{\mathrm{t}} = 2\hbar\omega_0\gamma_2 |B|^2$, and is assumed to be equal to the total power dissipated in the resonator. The heat balance equation reads

$$C\frac{\mathrm{d}T}{\mathrm{d}t} = Q_{\mathrm{t}} - W, \qquad (2)$$

where C is the thermal heat capacity, $W = H(T - T_0)$ is the heat transfer power to the coolant, and H is the heat transfer coefficient.

Coupling between eq. (1) and eq. (2) originates by the dependence of both the resonance frequency $\omega_0(T)$ and the damping rate $\gamma_2(T)$ of the driven mode on the resistance of the microbridge [14], which in turn

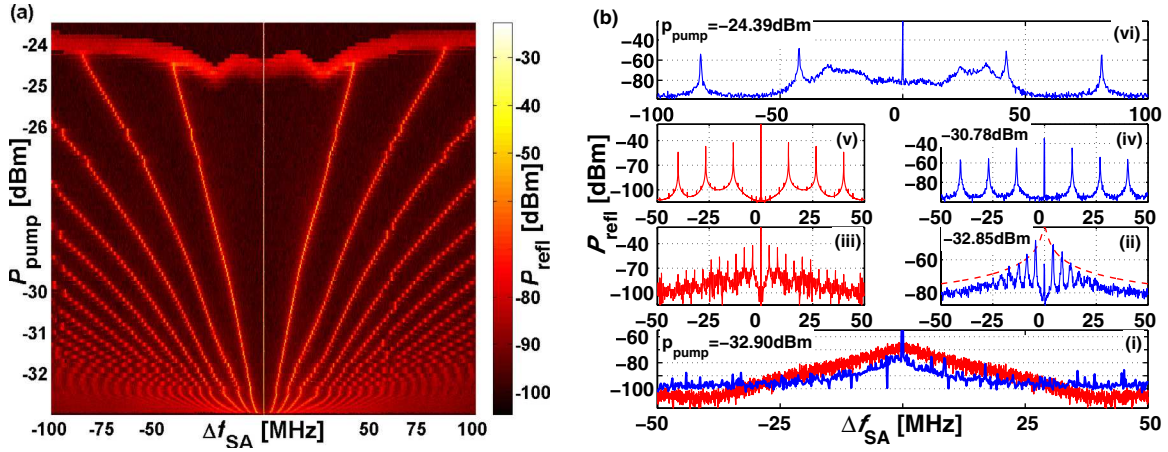

Fig. 2: (Color online) Typical experimental results of the SM phenomenon in the frequency domain. Panel (a) plots a color-map of the reflected power $P_{\rm refl}$ as a function of the pump power at the input of the resonator $P_{\rm pump}$ and the measured frequency $f_{\rm SA}$, centered on the pump frequency, which coincides with the resonance frequency $f_3 = 5.74\,\mathrm{GHz}$ ($\Delta f_{\rm SA} = f_{\rm SA} - f_3$). Panel (b), subplots (i), (ii), (iv), (vi), plot the same measurement at four different pump powers, corresponding to (i) the lower power threshold, (ii) and (iv) powers that are in the range of regular SM, and (vi) the upper power threshold. The red curve in subplot (ii), which has a Lorenzian shape, shows the spectral density of the SM sidebands as predicted theoretically by the model (eq. (26) of ref. [17]). The solid red curve in subplot (i) was obtained by numerically integrating the equations of motion of the model with a nonvanishing noise at the first power threshold and evaluating the spectral density [17]. Subplots (iii) and (v) were obtained by numerically integrating the equations of motion of the model for the noiseless case, at input powers corresponding to subplots (ii) and (iv) respectively, and calculating the spectral density. The parameters that were used in the simulation are summarized in table 1.

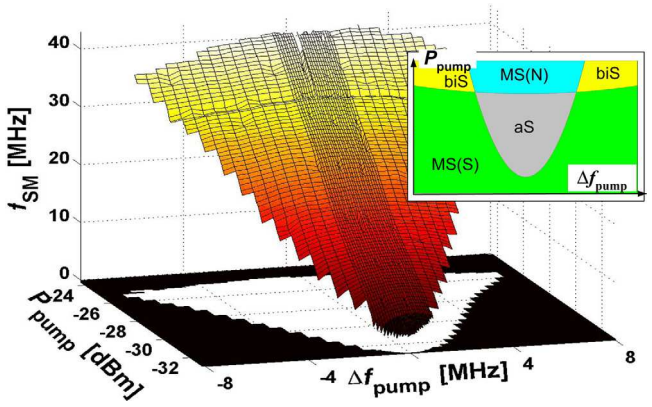

Fig. 3: (Color online) SM frequency $f_{\rm sm}$ as a function of the pump power and the pump frequency, centered on the resonance frequency $\Delta f_{\rm pump} = f_{\rm pump} - f_3$. The inset shows a schematic diagram of the stability zones of the resonator as a function of the pump power and frequency. The green, pale blue, yellow, and grey colors represent the SC monostable (MS(S)), NC monostable (MS(N)), bistable (biS), and astable (aS) zones, respectively.

depends on its temperature. We assume the simplest case, where this dependence is a step function that occurs at the critical temperature $T_{\rm c} \simeq 10\,\mathrm{K}$, namely $\omega_0 = \omega_{0\rm s}$ and $\gamma_2 = \gamma_{2\rm s}$ for $T < T_{\rm c}$, whereas $\omega_0 = \omega_{0\rm n}$ and $\gamma_2 = \gamma_{2\rm n}$ for $T > T_{\rm c}$. We further assume that all other parameters are temperature independent. In our previous publication [13] we have thoroughly investigated the dependence of the resonance modes on the resistance of the microbridge. We have shown that a resonance frequency can be smoothly shifted by gradually controlling the bridge resistance. In addition, the damping rate increases with the resistance up to a certain maximum, but then decreases back to approximately its original value, when the resistance is further increased.

Due to the step-like dependence of the resistance, and hence, of the heat generation, on the temperature of the microbridge [18], the system may have, in general, up to two locally stable steady states, corresponding to the SC and NC phases. The stability of each of these phases depends on both the power and frequency parameters of the injected pump tone. In general there exist four different stability zones (see inset in fig. 3) [17]. Two are mono-stable zones, where either the SC phase or the NC phase is locally stable. Another is a bistable zone, where both phases are locally stable [19,20]. The third is an astable zone, where none of the phases are locally stable, and consequently, the resonator is expected to oscillate between the two phases. The loaded Q-factor of the resonator in the SC and NC phases is approximately 2500 in the first case and 800 in the latter one. Thus, the two phases significantly differ in their reflection coefficients, and consequently, the oscillations translate into a modulation of the reflected pump tone. The mechanism introduced in this theoretical model is somewhat similar to one of the mechanisms which cause self-oscillations in an optical parametric oscillator [21].

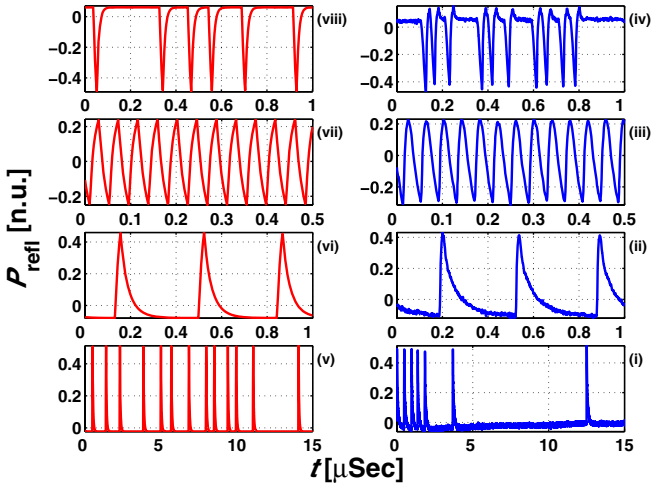

Fig. 4: Panels (i)–(iv) show typical experimental results of the SM phenomenon in the time domain. The reflected power is normalized by the value of the maximum peak-to-peak amplitude. AC coupling is employed in the measurement and thus a zero value represents the average measured power. Each panel refers to a different pump power range, (i) lower power threshold, (ii) and (iii) powers corresponding to regular SM. (iv) upper power threshold. Panels (v)–(viii) show numerical integration of eqs. (1) and (2) calculated for the above-mentioned four cases. The graphs are centered around their mean value and normalized by the value of the maximum peak-to-peak amplitude. In the simulation of the lower and upper thresholds (panels (v) and (viii)), a Gaussian thermal noise, corresponding to 4.2 K and 15 K temperatures was assumed respectively, whereas in the simulation of the regular SM, (panels (vi) and (vii)), the noise was disregarded. Supplementary video 2 (see footnote [2]) shows the SM in the time domain while gradually increasing the pump power from frame to frame. Each frame has a subplot similar to panels (i)–(iv), and a subplot similar to 2(*b*) panels (ii), (iv).

Further insight is gained by analyzing the dependence of the SM on the input power, as observed in the time domain (fig. 4). Below the lower power threshold the resonator is in the SC low reflective phase, where only a small portion of the injected power is reflected off the resonator. Once the pump power approaches the lower power threshold, sporadic spikes in the reflected power occur, as seen in subplot (i). Near the threshold the device is in sub-critical conditions and these spikes are caused by a stochastic noise which triggers transitions of the microbridge from the SC phase to the NC high reflective phase. During a transition the stored energy in the resonator is quickly discharged and dissipated. Consequently, after a quick warm-up the microbridge gradually cools down until eventually it switches back to the SC phase. As a result, the damping rate returns to its original value and a new recharging sequence begins. Once a spike is triggered, the noise has a negligible effect on the dynamics of the energy dissipation and recharging and therefore, the line-shapes of the various spikes are similar. This behavior can also be clearly observed in the simulation results, shown in subplot (v).

[2]Typical experimental results of the self-modulation in the time domain. Each frame has two subplots. The first plots the reflected power off the resonator as a function of time. The second plots the same measurement and a function of frequency, for reference. The frames are obtained while gradually increasing the pump power.

Table 1: Model parameters.

γ_1	8 MHz	$C =$	54 nJ cm^{-2} K^{-1}
γ_{2s}	15 MHz	H	12 W cm^{-2} K^{-1}
γ_{2n}	64 MHz	Q_t	1.7 μW
$\omega_{0s,n}/2\pi$	5.74 GHz	A_{eff}	1 μm^2

Regular SM of the reflected power (fig. 4(ii), (vi)) occurs when the pump power is set above the lower power threshold. In this case, the pump tone drives the resonator to the astable zone and the noise has a negligible influence. The dynamics of the oscillations is similar to the one just described where the energy buildup time is strongly dependent on the pump power. Thus, the oscillation frequency is faster for higher pump power values (fig. 4(iii), (vii)). The upper power threshold (fig. 4(vi)) resembles the lower one, but the SC and NC phases exchange roles. The resonator is in the NC high reflective phase, and noise-induced spikes temporarily drive it to the SC low reflective phase. The internal thermal noise in the upper threshold is stronger than in the lower one and, consequently, this threshold spreads over a wider power range.

The SM phenomenon is robust and occurs in all of our devices and at several resonance frequencies. The power level of the lower threshold mainly depends on the current density that flows through the microbridge; the higher the current density for a given input power, the lower the power threshold. The current density, in turn, mainly depends on the thickness of the resonator, and on the Q-factor and current distribution of the driven resonance mode. The thinner the device, the higher the current density that flows through the microbridge for a given input power. Higher Q-factors also result in higher current densities. As the variation in these two parameters can be rather large also the variation in the lower power threshold can be large, and indeed, lower power thresholds were measured in the range of $[-45\,\text{dBm}, -20\,\text{dBm}]$. The size of the power range where SM occurs depends on the difference between the damping rates γ_{2s} and γ_{2n}. This difference is also subjected to large variation and thus, the size of the power range varies between few and approximately twenty decibels.

The numerical results were calculated using the parameters summarized in table 1. The damping rates, the coupling coefficient, and the heating power Q_t were extracted from measurement results according to [13,19]. The thermal heat capacity C and the heat transfer coefficient were calculated analytically according to refs. [22,23]. A detailed derivation of these parameters can be found in ref. [17]. The effective size of the hotspot

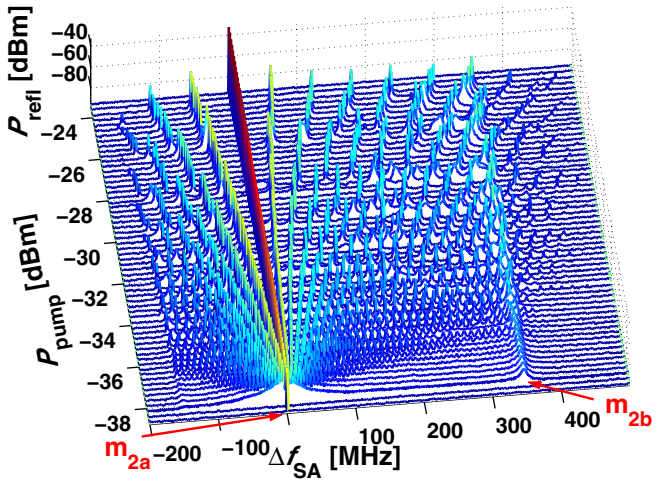

Fig. 5: (Color online) A typical SE measurement. The reflected power $P_{\rm refl}$ is measured as a function of the pump power $P_{\rm pump}$ and the measured frequency $f_{\rm SA}$ centered on the driven resonance frequency $f_{2\rm a}$ ($\Delta f_{\rm SA} = f_{\rm SA} - f_{2\rm a}$). In addition, it shows the self-excited resonance mode $\rm m_{2b}$.

$A_{\rm eff}$ can be calculated by using eq. (18) of ref. [19], $A_{\rm eff} \simeq Q_{\rm t}/H\,(T_c - T_0)$, which, for the given parameters, equals the width of the microbridge. By applying dc current-voltage measurements on the microbridge, as was done in [13], we estimate that the resistance of such a hotspot is approximately $10\,\Omega$, which is smaller than the characteristic impedance of the resonator. Therefore, such a hotspot would substantially increase the damping rate of the resonator, but would result in only a negligible resonance frequency shift [13], thus $\omega_{0\rm s} \cong \omega_{0\rm n}$.

In our measurements we find strong and correlated nonlinear phenomena accompanying the SM [12]. One of these phenomena is self-excitation (SE) of coupled resonance modes, which occurs when one of the modes is externally driven and undergoes self-oscillations. Typical SE results, measured with one of our devices, having resonance frequencies at $f_{2\rm a} = 4.55\,\rm GHz$ and $f_{2\rm b} = 4.9\,\rm GHz$, is shown in fig. 5. The resonator is driven by a monochromatic pump at frequency $f_{2\rm a}$. SE of the coupled mode ($\rm m_{2b}$) starts with the self-oscillations of the driven mode. At first the coupled mode experiences noise rise, and as the input power increases, SM of the emitted power from that mode is observed. Naturally, the sidebands which appear around the coupled mode are weaker than the ones around the directly driven mode, but as a result of the coupling, the sidebands around the primary mode become asymmetric.

In conclusion, we report on a novel nonlinear phenomenon where SM is generated in a SC microwave stripline resonator. This behavior is robust and occurs in all of our devices and at several resonance frequencies. A theoretical model according to which the SM originates by a thermal instability is introduced. In spite of its simplicity, the model exhibits a good quantitative agreement with the experimental results. Self-excitation of coupled resonance modes, which is one of few nonlinear phenomena that accompany the SM [12], is demonstrated.

* * *

We thank B. Yurke, R. Lifshitz, M. Cross, O. Gottlieb, and S. Shaw for valuable discussions. This work was supported by the German Israel Foundation, the Israel Science Foundation, the Deborah Foundation, the Poznanski Foundation, the Russel Berrie Nanotechnology Institute, and MAFAT.

REFERENCES

[1] Movshovich R., Yurke B., Kaminsky P. G., Smith A. D., Silver A. H., Simon R. W. and Schneider M. V., *Phys. Rev. Lett.*, **65** (1990) 1419.
[2] Yurke B. and Buks E., *J. Lightwave Tech.*, **24** (2006) 5054.
[3] Buks E. and Yurke B., *Phys. Rev. A*, **73** (2005) 023815.
[4] Segev E., Abdo B., Shtempluck O. and Buks E., ArXiv:quant-ph/0606099 (2006).
[5] Siddiqi I., Vijay R., Metcalfe M., Boaknin E., Frunzio L., Schoelkopf R. J. and Devoret M. H., *Phys. Rev. B*, **73** (2006) 054510.
[6] Wiesenfeld K. and McNamara B., *Phys. Rev. A*, **33** (1986) 629.
[7] Lee J. C., Oliver W. D., Berggren K. K. and Orlando T. P., ArXiv:cond-mat/0609561 (2006).
[8] Clorfeine A. S., *Appl. Phys. Lett.*, **4** (1964) 131.
[9] D'Aiello R. V. and Freedman S. J., *Appl. Phys. Lett.*, **9** (1966) 323.
[10] Peskovatskii S. A., Era I. I. and Barilovich O. I., *JETP Lett.*, **6** (1967) 227.
[11] Eru I. I., Kashchei V. A. and Peskovatskii S. A., *Sov. Phys. JETP*, **31** (1970) 416.
[12] Segev E., Abdo B., Shtempluck O. and Buks E., *Phys. Lett. A*, **366** (2007) 160.
[13] Arbel-Segev E., Abdo B., Shtempluck O. and Buks E., *IEEE Trans. Appl. Superconduct.*, **16** (2006) 1943.
[14] Saeedkia D., Majedi A. H., Safavi-Naeini S. and Mansour R. R., *IEEE Microwave Wireless Compon. Lett.*, **15** (2005) 510.
[15] Wiesenfeld K., *J. Stat. Phys.*, **38** (1985) 1071.
[16] Kravtsov Y. A., Bilchinskaya S. G., Butkovskii O. Y., Rychka I. A. and Surovyatkina E. D., *JETP*, **93** (2001) 1323; *Zh. Eksp. Teor. Fiz.*, **120** (2001) 1527.
[17] Segev E., Abdo B., Shtempluck O. and Buks E., *J. Phys. Cond. Matt.*, **19** (2007) 096206.
[18] Gurevich A. V. and Mints R. G., *Rev. Mod. Phys.*, **59** (1987) 941.
[19] Abdo B., Segev E., Shtempluck O. and Buks E., *IEEE Trans. Appl. Superconduct.*, **16** (2006) 1976.
[20] Abdo B., Segev E., Shtempluck O. and Buks E., *Phys. Rev. B*, **73** (2006) 134513.
[21] Suret P., Derozier D., Lefranc M., Zemmouri J. and Bielawski S., *Phys. Rev. A*, **61** (2000) 021805.
[22] Johnson M. W., Herr A. M. and Kadin A. M., *J. Appl. Phys.*, **79** (1996) 7069.
[23] Weiser K., Strom U., Wolf S. A. and Gubserm D. U., *J. Appl. Phys.*, **52** (1981) 4888.